Chemico-Biological Interactions 189 (2011) 146–152

Contents lists available at ScienceDirect

Chemico-Biological Interactions

journal homepage: www.elsevier.com/locate/chembioint

Regio- and stereoselective oxidation of propranolol enantiomers by human CYP2D6, cynomolgus monkey CYP2D17 and marmoset CYP2D19

Shizuo Narimatsu[a,*], Toshiyuki Nakata[a], Takeshi Shimizudani[a], Kenjiro Nagaoka[a], Hironori Nakura[a], Kazufumi Masuda[b], Takashi Katsu[a], Akiko Koeda[c], Shinsaku Naito[d], Shigeru Yamano[e], Atsuro Miyata[f], Nobumitsu Hanioka[a]

[a] Graduate School of Medicine, Dentistry and Pharmaceutical Sciences, Okayama University, 1-1-1 Tsushima-naka, Kita-ku, Okayama 700-8530, Japan
[b] School of Pharmacy, Shujitsu University, 1-6-1 Nishigawara, Naka-ku, Okayama 703-8516, Japan
[c] Ina Research Inc., 1248-188 Nishiminowa, Ina, Nagano 399-4501, Japan
[d] Otsuka Pharmaceutical Factory Inc., Naruto, Tokushima 772-8601, Japan
[e] Faculty of Pharmaceutical Sciences, Fukuoka University, 8-19-1 Nanakuma, Jonan-ku, Fukuoka 814-0180, Japan
[f] Kagoshima University, Graduate School of Medicine and Dentistry, 8-35-1 Sakuragaoka, Kagoshima 890-8520, Japan

ARTICLE INFO

Article history:
Received 16 September 2010
Received in revised form
22 November 2010
Accepted 8 December 2010
Available online 22 December 2010

Keywords:
Propranolol enantiomer
CYP2D6
CYP2D17
CYP2D19
Regioselectivity
Stereoselectivity

ABSTRACT

Toxic and pharmacokinetic profiles of drug candidates are evaluated in vivo often using monkeys as experimental animals, and the data obtained are extrapolated to humans. Well understanding physiological properties, including drug-metabolizing enzymes, of monkeys should increase the accuracy of the extrapolation. The present study was performed to compare regio- and stereoselectivity in the oxidation of propranolol (PL), a chiral substrate, by cytochrome P450 2D (CYP2D) enzymes among humans, cynomolgus monkeys and marmosets. Complimentary DNAs encoding human CYP2D6, cynomolgus monkey CYP2D17 and marmoset CYP2D19 were cloned, and their proteins expressed in a yeast cell expression system. The regio- and stereoselective oxidation of PL enantiomers by yeast cell microsomal fractions were compared. In terms of efficiency of expression in the system, the holo-proteins ranked CYP2D6 ≒ CYP2D17 ≫ CYP2D19. This may be caused by the bulky side chain of the amino acid residue at position 119 (leucine for CYP2D19 vs. valine for CYP2D6 and CYP2D17), which can disturb the incorporation of the heme moiety into the active-site cavity. PL enantiomers were oxidized by all of the enzymes mainly into 4-hydroxyproranolol (4-OH-PL), followed by 5-OH-PL and N-desisopropylpropranolol (NDP). In the kinetic analysis, apparent K_m values were commonly in the μM range and substrate enantioselectivity of *R*-PL < *S*-PL was observed in both K_m and V_{max} values for the formation of the three metabolites from PL enantiomers. The activity to produce NDP tended to be higher for the monkey enzymes, particularly CYP2D17, than for the human enzyme. These results indicate that in the oxidation of PL enantiomers by CYP2D enzymes, stereoselectivity is similar but regioselectivity is different between humans and monkeys.

1. Introduction

Since various human tissues and recombinant enzymes have become available, the metabolic profiles of drug candidates can be predicted fairly accurately in experiments in vitro. However, toxic and pharmacokinetic profiles of drug candidates should still be evaluated in vivo using experimental animals and the data obtained extrapolated to humans. In this context, monkeys such as cynomolgus monkeys, rhesus monkeys and marmosets are superior to non-primates such as rodents, rabbits, and dogs as experimental animal species. Cynomolgus monkeys are rather big (5–10 kg in body weight) as compared with marmosets (200–300 g), which affects handling and feeding. Though cynomolgus monkeys and rhesus monkeys have been used extensively in research into drug metabolism and toxicology, relatively little data has been obtained from marmosets.

Drug metabolism is divided into phase I reactions consisting of oxidation, reduction and hydrolysis and phase II reactions consisting of various kinds of conjugation. The oxidation catalyzed by cytochrome P450s (CYPs) makes up about 80% of phase I reactions [1]. CYPs compose a superfamily of hemethiolate enzymes, and over 10,000 CYPs from animals, birds, fish, plants, microor-

Abbreviations: CYP, cytochrome P450; PL, propranolol; X-OH-PL, X-hydroxypropranolol; NDP, N-desisopropylpropranolol; 4-OH-BTL, 4-hydroxybunitrolol; PVDF, polyvinylidene difluoride; PCR, polymerase chain reaction; SRS, substrate recognition site.

* Corresponding author. Tel.: +81 86 251 7942; fax: +81 86 251 7942.
E-mail address: shizuo@pharm.okayama-u.ac.jp (S. Narimatsu).

0009-2797/$ – see front matter © 2010 Elsevier Ireland Ltd. All rights reserved.
doi:10.1016/j.cbi.2010.12.014

ganisms etc. are known to exist [2]. Major isoenzymes of CYP1, 2 and 3 are responsible for drug metabolism in humans, namely CYP1A1/2, -2A6, -2B6, 2C8, -2C9, -2C19, -2D6, -2E1 and -3A4/5 [3]. CYP2D6 is clinically important because it contributes as the major enzyme to the oxidation of 15% of clinically prescribed medicines [4], though it accounts for only about 2% of all hepatic CYPs [5]. CYP2D6 shows extensive genetic polymorphism, and some 80 allelic variants have been reported to date [6], resulting in variation in drug-response phenotypes such as poor, intermediate, extensive and super-extensive metabolizers [4]. Cynomolgus monkeys and marmosets also have many CYPs [2] including CYP2D enzymes; CYP2D17 for cynomolgus monkeys [7] and CYP2D19 [8] and CYP2D30 [9] for marmosets.

Propranolol (PL) is a classical adrenoceptor blocking agent used clinically to treat arrhythmia and hypertension. PL has an asymmetric carbon atom in its side-chain, yielding the enantiomers *R*-PL and *S*-PL. Though *S*-PL has much more pharmacological activity as a β-blocker than *R*-PL [10], PL is given as a racemate. PL undergoes extensive metabolism in humans as shown in Fig. 1. For example, it is oxidized at the aromatic 4- and 5-positions mainly by CYP2D6 yielding 4-hydroxypropranolol (4-OH-PL) and 5-OH-PL, respectively, whereas the oxidation of the PL side-chain is mainly catalyzed by CYP1A2 giving N-desisopropylpropranolol (NDP) [11]. The oxidative metabolites as well as the parental compound are the substrates for UDP-glucuronosyltransferases and sulfotransferases [12,13]. PL is thus a useful substrate to study species differences in the regio- and stereoselective metabolism by CYP and conjugation enzymes.

Recently, we examined the oxidation of PL enantiomers by microsomal fractions from cynomolgus monkey and marmoset livers, and compared it with that by a human liver microsomal fraction [14]. As a result, we obtained experimental evidence that CYP2D enzymes are involved not only in the ring hydroxylation at the 4- and 5-positions but also in the side-chain N-desisopropylation in the monkey liver microsomal fractions [14]. In the present study, we expressed cynomolgus monkey CYP2D17 and marmoset CYP2D19 as well as human CYP2D6 in yeast cells, and compared the oxidation of PL enantiomers by yeast cell microsomal fractions among monkeys and humans.

2. Materials and methods

2.1. Materials

PL enantiomers as hydrochlorides were obtained from Sigma–Aldrich (St. Louis, MO); 4-OH-PL and 5-OH-PL as hydrochlorides from C/D/N Isotopes Inc. (Quebec, Canada); NDP as a hydrochloride from AstraZenaca (Cheshire, England); and 4-hydroxybunitrolol (4-OH-BTL) as a hydrochloride from Nippon Boehringer Ingelheim Co. (Hyogo, Japan). The RNeasy Mini kit, QIA shredder, and MiniElute Gel Extraction kit were purchased from Qiagen (Heiden, Germany). The RNA PCR kit v3.0, DNA ligation kit v2.1, Taq DNA polymerase, calf intestinal alkaline phosphatase and HindIII were from Takara Bio (Ohtsu, Japan); pGEM-T vector and T4 DNA ligase from Promega (Madison, WI); KOD-plus DNA polymerase from Toyobo (Osaka, Japan); Quantum Prep Plasmid Miniprep kit and polyvinylidene difluoride (PVDF) membrane from BioRad (Hercules, CA); and BigDye terminator cycle sequencing reaction kit v3.1 from Applied Biosystems (Foster City, CA). Horse radish peroxidase-conjugated anti-rabbit IgG was obtained from ICN Pharmaceuticals Inc. (Costa Mesa, CA). Enhanced chemiluminescence-plus reagents were from GE Healthcare Bio-Sciences Inc. (Little Chalfont, UK). Livers from adult male common marmosets were supplied by Professor Atsuro Miyata of Kagoshima University (Kagoshima, Japan). Livers from adult male cynomolgus monkeys were from Ina Research Co. Ltd. (Ina, Japan). Microsomal fractions from cynomolgus monkey and marmoset livers were prepared according to published methods [15]. Pooled human liver microsomal fractions were obtained from BD Biosciences (San Jose, CA).

Table 1
Primers used for the amplification of CYP2D17 cDNA.

Primer	Sequence	T_m (°C)	Length (bp)
CYP2D17-F1	ATGGAGCTAGATGCACTGGTGCCCCTGGC	69.0	29
CYP2D17-R1	CTAGCGGGGCACAGCACAAAGCTCATAGG	69.0	29
CYP2D17-F2	AAGCTT*AAAAAA*ATGGAGCTAGATGCACTG	59.2	30
CYP2D17-R2	AAGCTTTCTAGCGGGGCACAGCACA	63.9	25

Underlined and italic letters indicate restriction enzyme sites and the Kozak sequence, respectively.

2.2. Cloning of cDNA encoding CYP2D17

Total RNA was extracted from cynomolgus monkey liver using the RNeasy minikit and QIA shredder according to the manufacturer's instructions. The total RNA was reverse-transcribed to cDNA using the RNA PCR kit v3.0. The full-length cDNA encoding CYP2D17 was amplified by PCR from single-strand cDNA templates using CYP2D17-F1 and -R1 as primers (Table 1). These primers were designed based on the nucleotide sequence in the flanking regions of CYP2D17 cDNA (GenBank accession number Q29488). The PCR reaction mixture contained 1× PCR buffer, 0.2 mM dNTPs, each primer at 0.2 μM, 1.5 mM $MgSO_4$, and 1 U of KOD plus DNA polymerase in a final volume of 50 μL. The PCR consisted of 30 cycles with denaturation at 94 °C for 15 s, annealing at 65 °C for 30 s and extension at 68 °C for 100 s. The PCR product was isolated and purified by agarose electrophoresis, and the 5′- and 3′-ends of the coding region were sequenced in both the forward and reverse directions. The full-length cDNA obtained was modified by amplification with CYP2D17-F2 and -R2 as primers (Table 1). The PCR was performed with a similar reaction medium to that as described above though the annealing temperature was 58 °C. The PCR product was isolated and purified by agarose electrophoresis. The PCR product was introduced into the pGEM-T vector after A-tailing and sequenced in both the forward and reverse directions. A DNA fragment corresponding to CYP2D17 was cut from the pGEM-T vector with HindIII, and subcloned into pGYR1 digested with the same restriction enzyme. The insert of the plasmid was sequenced to verify the correct orientation with respect to the promoter for pGYR1. Construction of the expression plasmids containing each of CYP2D6 and CYP2D19 was described previously [9].

2.3. Expression of CYP2D enzymes

Saccharomyces cerevisiae AH22 was transformed with pGYR1 containing each of the CYP2D cDNAs by the lithium acetate method, and the culture of yeast transformants thus obtained was performed as described previously [16]. Microsomal fractions were prepared from yeast cells expressing the CYP2D enzymes by methods reported previously [16]. The fractions were diluted to a protein concentration of 5.0 mg/mL with 100 mM potassium phosphate buffer (pH 7.4) containing 0.4% Emulgen 911 and 20% glycerol. Total holo-CYP content was measured spectrophotometrically by the method of Omura and Sato [17] using 91 $mM^{-1}\,cm^{-1}$ as the absorption coefficient. Appropriate portions of the yeast cell microsomal fractions together with microsomal fractions from human, cynomolgus monkey and marmoset livers were subjected to sodium dodecyl sulfate-polyacrylamide gel electrophoresis using a 10% slab gel. Following the electrophoresis, proteins on the gel were electroblotted to a PVDF membrane, and analyzed by Western

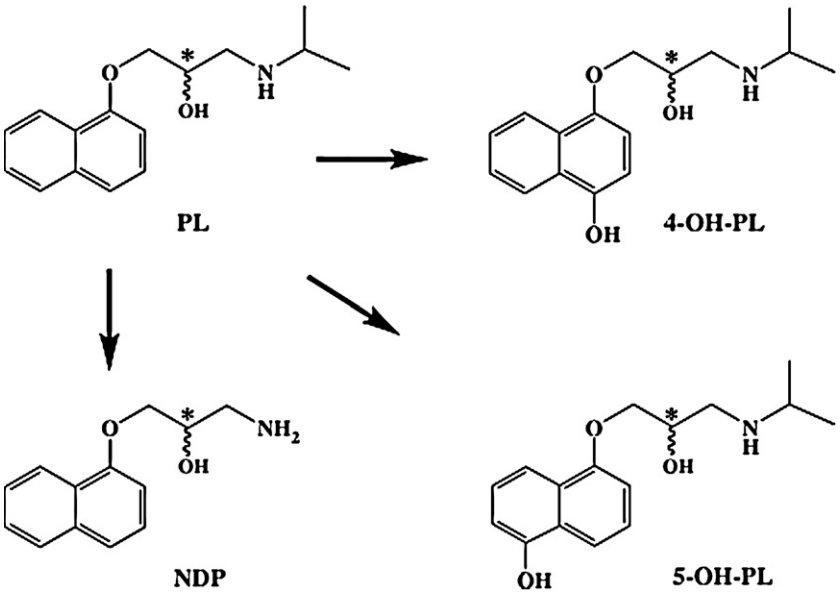

Fig. 1. Primary oxidation pathways of PL in humans. *Asymmetric carbon atom.

blotting according to published methods [18] employing polyclonal antibodies raised against CYP2D6 (rabbit antiserum) prepared in this lab as the primary antibody and peroxidase-conjugated goat anti-rabbit IgG as the secondary antibody.

2.4. Enzyme assay

The oxidative activities of PL enantiomers in the yeast cell microsomal fractions were measured as described previously [14]. Briefly, an ice-cold reaction mixture containing 10 mM G-6-P, 1 IU of G-6-P dehydrogenase, 1 mM $NADP^+$, 5 mM $MgCl_2$, 0.2–200 μM *R*-PL or *S*-PL and 100 mM potassium phosphate buffer (pH 7.4) in a final volume of 500 μL was preincubated at 37 °C for 1 min. The reaction was started by adding the microsomal fraction (0.08, 0.05 and 0.5 mg protein/mL for CYP2D6, CYP2D17 and CYP2D19, respectively) and stopped by adding 1 mL of 1 M aqueous NaOH containing sodium bisulfite (25 mg/mL) as an antioxidant and mixing vigorously. Then, 4-OH-BTL (200 pmol) as the internal standard was added, and PL and metabolites were extracted into ethyl acetate (4 mL) by shaking at room temperature. The organic layer was evaporated, and the residue was dissolved in 100 μL of the mobile phase of HPLC described below. Calibration curves were made by adding known amounts of PL metabolites to the incubation medium and by extracting the metabolites without incubation in the same manner as above. Protein concentrations were measured by the method of Lowry et al. [19] using bovine plasma albumin as a standard. The HPLC system consisted of an LC-10AD pump, a RF-10A fluorescence detector, a CTO-10A column oven, an SIL-10A injector and a CBM-10A integrator (Shimadzu Co., Kyoto, Japan). The conditions were as follows: column, Inertsil ODS-3 (4.6 mm i.d. × 250 mm, 5 μm, GL Science Co. Tokyo, Japan); column temperature, 30 °C; mobile phase, 10 mM ammonium acetate buffer (pH 4.0)/methanol (59:41 by volume); flow rate, 1.0 mL/min; detection, fluorescence at 310/380 nm for excitation/emission wavelengths. In preliminary experiments, the linearity in the metabolite formation was confirmed for protein concentrations and incubation time.

2.5. Data analysis

Kinetic parameters (apparent K_m and V_{max} values) were estimated by analyzing Michaelis–Menten plots using the computer program Prism v5.0 (GraphPad Software, San Diego, CA). Intrinsic clearance (CL_{int}) was determined as the ratio V_{max}/K_m. All values are expressed as the mean ± S.D. for three separate experiments with independent preparations. Statistical comparisons were made with Student's *t*-test or Tukey's test using Prism v5.0, and a difference was considered significant when the *p*-value was <0.05.

2.6. Molecular modeling

The homology models of CYP2D17 and CYP2D19 were constructed using Swiss Model (http://swissmodel.exspasy.org/) employing the crystallographic data of CYP2D6 (PDB ID, 2F9Q). Hydrogen atoms were added to the models using the Biopolymer module of Insight II software (Molecular Simulation Inc., San Diego, CA). A heme moiety and six peptides as substrate recognition sites (SRSs) were extracted; from 101 to 123 as SRS1, 205 to 223 as SRS2, 236 to 247 as SRS3, 296 to 311 as SRS4, 367 to 376 as SRS5 and 479 to 485 as SRS6. Energy optimization of the models was performed using Insight II/Discover as described previously [20]. The active site models were drawn using RasMol v2.6-ucb-1.0 [20].

3. Results

3.1. Expression of CYP2D enzymes in yeast cells

Yeast cell microsomal fractions expressing CYP2D6 and CYP2D17 yielded typical reduced carbon monoxide (CO)-difference spectra, while the CYP2D19 fraction showed a spectrum having a low Soret peak at 450 nm (Fig. 2). The amounts of the recombinant enzymes were 39.1 ± 11.5, 63.3 ± 18.8 and 4.38 ± 0.83 pmol/mg protein for CYP2D6, CYP2D17 and CYP2D19, respectively. The concentration of CYP2D19 was significantly lower than that of CYP2D6 or CYP2D17. Western blot analysis using the polyclonal antibody against CYP2D6 gave a single protein band for each sample (human, cynomolgus monkey and marmoset liver microsomal fractions, and microsomal fractions from yeast cells expressing human, cynomolgus monkey and marmoset recombinant CYP2D enzymes) with a similar migration profile (Fig. 3). The protein bands in the liver microsomal fractions of cynomolgus monkeys and marmosets were strongly stained whereas staining of the protein band of the human

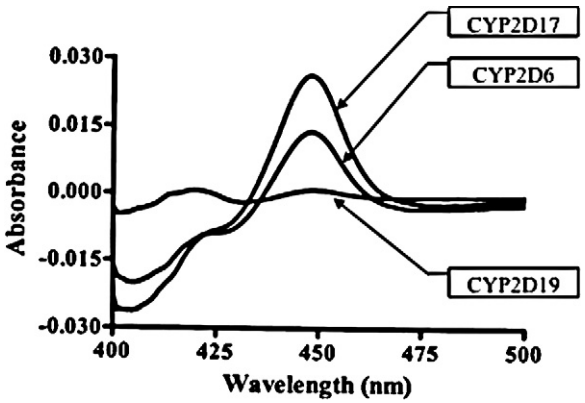

Fig. 2. Typical reduced CO-difference spectra of microsomal fractions from yeast cells expressing CYP2D6, CYP2D17 and CYP2D19. The microsomal protein concentration was 10 mg/mL.

sample was relatively weak. In contrast, the protein band for the marmoset enzyme was weak compared with the bands for the human and cynomolgus monkey enzymes.

3.2. Oxidation activity of PL enantiomers by recombinant CYP enzymes

Employing PL enantiomers (each 100 μM) as substrates, functions of the three recombinant CYP2D enzymes were examined. As shown in typical HPLC chromatograms (Fig. 4), three PL metabolites were eluted at the retention times of 4.6 min for 5-OH-PL, 5.6 min for 4-OH-PL and 10.3 min for NDP, which were formed from both PL enantiomers. The internal standard (4-OH-BTL) and the substrates (PL enantiomers) were eluted at the retention times of 3.9 min and 15.8 min, respectively. Under the fluorescence HPLC conditions employed (excitation/emission wavelengths = 310/380 nm), the peak heights ratio of 5-OH-PL:4-OH-PL:NDP in the same amounts is 10:1:4, which was calculated from the calibration curves. This is due to the difference in the fluorescence intensities among the three metabolites.

In the case of CYP2D6 (Fig. 4A), the peak heights of the metabolites formed were 5-OH-PL > 4-OH-PL > NDP. The peak heights for all three metabolites showed a tendency of *R*-metabolites < *S*-metabolites (Fig. 4A and Table 2), meaning that the oxidation activities of *S*-PL are higher than those of *R*-PL. In the case of CYP2D17 (Fig. 4B), the peak heights of the metabolites formed were NDP > 4-OH-PL > 5-OH-PL. The peak heights for *R*-5-OH-PL and *R*-NDP tended to be higher than those of corresponding *S*-metabolites, whereas the peak heights for 4-OH-PL enantiomers were almost the same (Table 2). In the case of CYP2D19 (Fig. 4C), the peak heights of the metabolites were 5-OH-PL > 4-OH-PL > NDP, and the R/S ratio in the metabolite formation was similar to the case of CYP2D17 (Table 2).

Fig. 3. Western blot analysis of microsomal fractions from human and monkey livers, and from yeast cells expressing human and monkey recombinant enzymes. Typical results for pooled microsomes from three independent preparations are shown. The microsomal protein levels were 20 μg/lane for liver microsomes and 0.5 μg/lane for yeast cell microsomes. HLM, human liver microsomes; CLM, cynomolgus liver microsomes, MLM, marmoset liver microsomes, 2D6, CYP2D6; 2D17, CYP2D17; 2D19, CYP2D19. Conditions are given in Section 2.

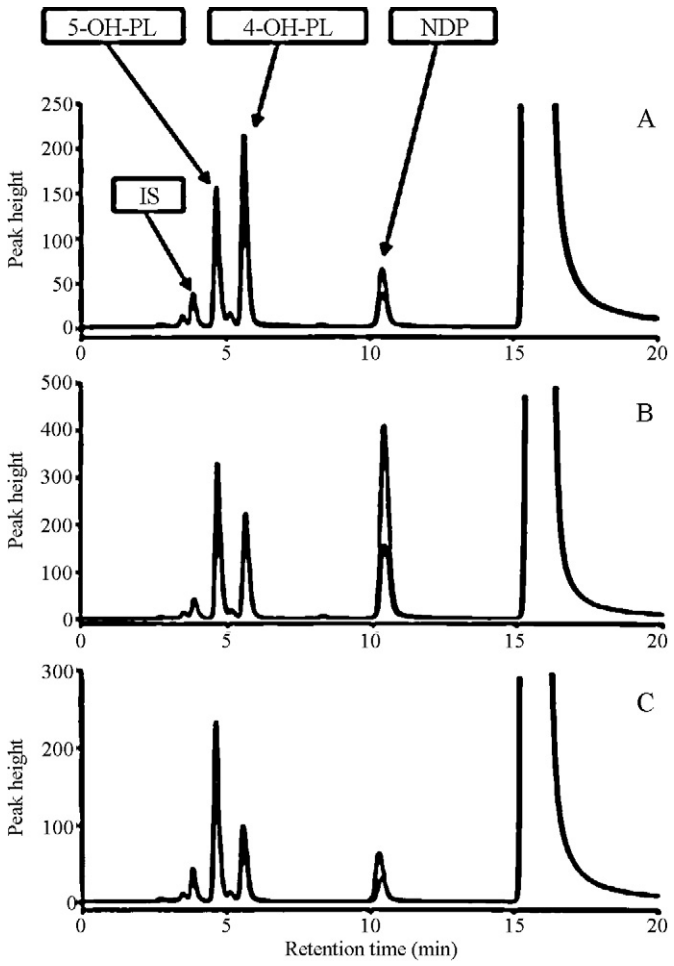

Fig. 4. Typical HPLC chromatograms showing the formation of 4-OH-PL, 5-OH-PL and NDP from PL enantiomers by human, cynomolgus monkey and marmoset CYP2D enzymes. Thin line, formed from *S*-PL; thick line, formed from *R*-PL. (A) HM-CYP2D6, (B) CYP2D17 and (C) CYP2D19 as enzyme sources. IS, internal standard (4-OH-BTL). The substrate concentration used was 100 μM. HPLC conditions are given in Section 2.

Table 2
Comparison of metabolites formed from PL enantiomers by recombinant CYP2D enzymes.

Metabolite	Retention time (min)	Peak height[a]	*R*/*S* ratio[b]
CYP2D6			
R-5-OH-PL	4.62	103	0.68
S-5-OH-PL	4.62	151	
R-4-OH-PL	5.59	138	0.68
S-4-OH-PL	5.59	203	
R-NDP	10.28	34	0.57
S-NDP	10.28	60	
CYP2D17			
R-5-OH-PL	4.62	233	0.70
S-5-OH-PL	4.62	332	
R-4-OH-PL	5.59	216	1.04
S-4-OH-PL	5.59	207	
R-NDP	10.28	164	0.39
S-NDP	10.28	418	
CYP2D19			
R-5-OH-PL	4.62	140	0.63
S-5-OH-PL	4.62	222	
R-4-OH-PL	5.59	93	1.00
S-4-OH-PL	5.59	93	
R-NDP	10.28	31	0.50
S-NDP	10.28	62	

[a] Peak height values represent the detector response (μV) in the HPLC (Fig. 3).
[b] *R*/*S* ratio was calculated by dividing the peak height of the *R*-metabolite with that of the corresponding *S*-metabolite.

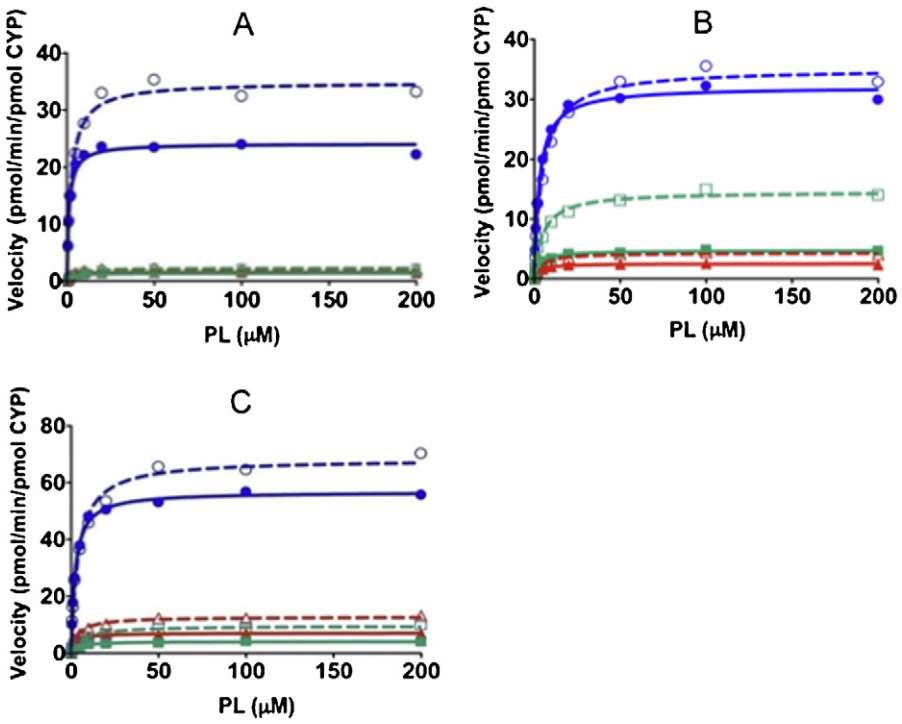

Fig. 5. Typical Mechaelis–Menten plots for the formation of 4-OH-PL, 5-OH-PL and NDP from PL enantiomers by human, cynomolgus monkey and marmoset CYP2D enzymes. (A)–(C) shows CYP2D6, CYP2D17 and CYP2D19, respectively. Circles, 4-OH-PL; triangles, 5-OH-PL; squares, NDP; open symbols and broken lines, formed from *S*-PL; closed symbols and solid lines, formed from *R*-PL. Experimental conditions are given in Section 2.

3.3. Kinetic analysis of the oxidation of PL enantiomers by recombinant CYP2D enzymes

The formation of all metabolites from PL enantiomers fitted to the Michaelis–Menten plots (Fig. 5). These plots demonstrated that the major metabolite was 4-OH-PL for all CYP2D enzymes, and NDP formed as a second major metabolite only for CYP2D17. The kinetic parameters are summarized in Table 3. There was no significant difference in the apparent K_m values among the three recombinant enzymes. From the view point of regioselectivity, the V_{max} values for the formation of 4-OH-PL and 5-OH-PL from both PL enantiomers were significantly higher for CYP2D19 than for CYP2D6 and CYP2D17. Furthermore, the V_{max} value for the formation of NDP from *S*-PL was significantly higher for CYP2D17 than for CYP2D6. The CL_{int} values for the formation of 5-OH-PL by CYP2D19 were significantly higher than the corresponding values for the human and cynomolgus monkey enzymes. On the other hand, the CL_{int} values for the formation of 4-OH-PL by the marmoset enzyme were significantly higher than for CYP2D17. From the view point of stereoselectivity, substrate enantioselectivity of *R*-PL < *S*-PL was observed for the K_m and V_{max} values for the formation of all metabolites from PL enantiomers by all of the recombinant enzymes.

4. Discussion

We previously examined the oxidative metabolism of PL enantiomers by liver microsomal fractions from cynomolgus monkeys and marmosets, and found that the kinetic profiles were considerably different between the two monkey species [14]. However, we obtained some lines of experimental evidence that not only PL aromatic ring hydroxylation at the 4- and 5-positions but also side-chain N-desalkylation was mediated by monkey CYP2D enzymes, because the formation of the three metabolites from PL enantiomers by the monkey liver microsomal fractions was inhibited by a polyclonal CYP2D6 antibody and quinidine, a specific inhibitor of CYP2D6 [14]. In the present study, we cloned cDNA encoding CYP2D17 from the total RNA fractions from cynomolgus monkey liver, and expressed its protein in the yeast cell expression system. Then, the oxidation of PL enantiomers by the recombinant CYP2D17 was compared with that by the human CYP2D6 and marmoset CYP2D19 expressed in the same system as described previously [9].

Functional CYP levels in yeast cell microsomal fractions were determined based on reduced CO-difference spectra. The level of the CYP2D19 holo-protein was significantly lower than levels of the human and cynomolgus monkey CYP2D enzymes. Similar results were obtained in our previous study in which the level of CYP2D19 was much lower than that of CYP2D6 [9]. As shown in Fig. 2, the peak heights at 450 and 420 nm were almost the same in the reduced CO-difference spectrum for the recombinant CYP2D19. A similar tendency was observed for the other two recombinant CYP2D19 samples (data no shown). Considering the absorbance coefficients of 91 and 111 $mM^{-1}\,cm^{-1}$ for cytochromes P450 and P420, respectively, in mammalian liver microsomes [17,22], the total contents of functional (P450) and denatured (P420) CYP2D19 in yeast cell microsomal fractions were estimated to be less than 15% and 25% those of functional CYP2D17 and 2D6, respectively.

To search for a possible cause, we constructed a homology model of CYP2D19 by Swiss Model on the website employing crystallographic data of CYP2D6 in the present study. The active-site structure consisting of six SRSs and the heme moiety was extracted from the whole conformation of CYP2D19 and carefully compared with that of CYP2D6 The possibility arises that an amino acid residue, leucine, at position 119 may cause the low efficiency in the expression of the holo-protein for CYP2D19. That is, the amino acid at the corresponding position is valine for CYP2D6 and CYP2D17, both of which yield typical reduced CO-difference spectra (Fig. 2). The side chain (isobutyl group) of leucine is larger than that (isopropyl) of valine as shown in Fig. 6, indicating that appropriate

Table 3
Kinetic parameters for the oxidation of PL enantiomers by microsomal fractions from yeast cells expressing human, cynomolgous monkey and marmoset CYP2D enzymes.

Metabolite	K_m (μM)			V_{max} (pmol/min pmol CYP)			CL_{int} (μL/min pmol CYP)		
	R	*S*	*R/S*	*R*	*S*	*R/S*	*R*	*S*	*R/S*
CYP2D6									
4-OH-PL	1.25 ± 0.41	2 .43 ± 0.68	0.51	24.2 ± 5.7	34.9 ± 7.4 0	0.69	20.1 ± 3.9	14.6 ± 1.6	1.38
5-OH-PL	1.06 ± 0.73	2.56 ± 0.65	0.62	1.60 ± 0.42	2.20 ± 0.53	0.73	1.11 ± 0.38	0.86 ± 0.02	1.28
NDP	2.52 ± 1.22	3.52 ± 0.78	0.78	1.39 ± 0.50	2.30 ± 0.66	0.61	0.57 ± 0.09	0.66 ± 0.19	0.87
CYP2D17									
4-OH-PL	2.99 ± 0.38*	5.04 ± 1.22*	0.59	32.0 ± 8.5	35.2 ± 11.5	0.91	11.1 ± 4.5	7.26 ± 4.32	1.46
5-OH-PL	2.88 ± 0.33	4.51 ± 1.07	0.64	2.49 ± 0.68	4.30 ± 1.47	0.58	0.89 ± 0.36	1.04 ± 0.61	0.86
NDP	3.14 ± 0.30	5.25 ± 1.22*	0.60	4.70 ± 2.06	14.6 ± 6.40*	0.32	1.51 ± 0.70	3.12 ± 2.23	0.49
CYP2D19									
4-OH-PL	2.30 ± 0.71	3.97 ± 1.28	0.58	57.0 ± 10.4*,‡	68.3 ± 9.6*,‡	0.83	25.4 ± 3.2*	17.8 ± 3.0‡,#	1.42
5-OH-PL	2.32 ± 0.73	3.81 ± 1.22	0.61	7.13 ± 2.27*,‡	12.8 ± 3.8*,‡	0.56	3.07 ± 0.07*,‡	3.41 ± 0.51*,‡	0.90
NDP	4.54 ± 3.55	6.32 ± 2.66	0.72	4.23 ± 0.92*,#	9.64 ± 1.64#	0.44	1.24 ± 0.59*,‡	1.63 ± 0.41*,‡	0.76

Each value represents the mean ± S.D. for three separate experiments with three independent preparations. Significant differences were calculated with Tukey's test for species difference or Student's *t*-test for enantioselectivity.
* $p < 0.05$ compared with CYP2D6.
# $p < 0.05$ compared with *R*-PL.
‡ $p < 0.05$ compared with CYP2D17.

incorporation of the heme moiety may be disturbed with the bulky side-chain of Leu-119 during the biosynthesis of the CYP2D19 protein.

In the Western blot analysis of liver microsomal fractions (Fig. 3), however, marmoset liver microsomes as well as cynomolgus monkey liver microsomes showed a thick protein band that immunochemically reacted with the polyclonal antibody raised against CYP2D6. Recently, Uno et al. [21] succeeded in cloning a cDNA encoding a novel CYP2D44 from cynomolgus monkey liver and characterized its enzymatic properties. We also demonstrated previously the expression of two CYP2D genes in marmoset livers, i.e., CYP2D19 and CYP2D30 were found to be expressed in marmoset livers supplied from Kagoshima University and from Kyoto University, respectively [9]. In the present study, we used marmoset livers supplied from Kagoshima University, and so the possibility arises that an unknown CYP2D enzyme, like cynomolgus monkey CYP2D44, may express together with CYP2D19 in marmoset livers obtained from Kagoshima University.

In general, the kinetic profiles for the oxidation of PL enantiomers were similar among the three recombinant enzymes; (1) apparent K_m values were around several μM, (2) substrate enantioselectivity of *R*-PL < *S*-PL was observed in both the K_m and V_{max} values for the three metabolites formed from PL enantiomers, and (3) the most abundant metabolite was commonly 4-OH-PL for all of the recombinant enzymes. On the other hand, considerable differences were observed in the following points; (4) compared with CYP2D6 and CYP2D17, CYP2D19 had higher activity for the formation of 4-OH-PL and 5-OH-PL, and (5) the NDP-forming activity, particularly from *S*-PL, was much higher in CYP2D17 than in CYP2D6. Furthermore, the kinetic profiles of the PL oxidation by the recombinant enzymes were similar to those by liver microsomal fractions from humans, cynomolgus monkeys and marmosets obtained in our previous studies [14], i.e., the K_m values for the recombinant enzymes were close to the values of low-K_m phases for the liver microsomal fractions. However, *S*/*R* ratios in the K_m values were slightly different between the recombinant enzymes and the liver microsomal fractions [14], which may be due to involvement of some other CYP enzyme(s) in addition to CYP2D6, CYP2D17 or CYP2D19 in PL oxidation in each liver microsomal fraction.

Employing the crystal structure of CYP2D6, we constructed homology models of CYP2D19 and CYP2D17 by the Swiss Model, and performed docking simulations on a personal computer using the Insight II/Discover program. We did not obtain any potential docking model, which can explain why the NDP-forming activity is higher in CYP2D17 and/or CYP2D19 than in CYP2D6. Further studies are necessary to elucidate mechanism(s) causing the species differences in DNP formation between human and monkey enzymes together with the possibility of the existence of another CYP2D enzyme in marmoset livers.

In summary, cynomolgus monkey, marmoset and human CYP2D enzymes were expressed in a yeast cell system, and the regio- and stereoselective oxidations of PL enantiomers by yeast cell microsomal fractions were compared. In efficiency of expression in the system, the ranking was CYP2D6 ≒ CYP2D17 ≫ CYP2D19. PL enan-

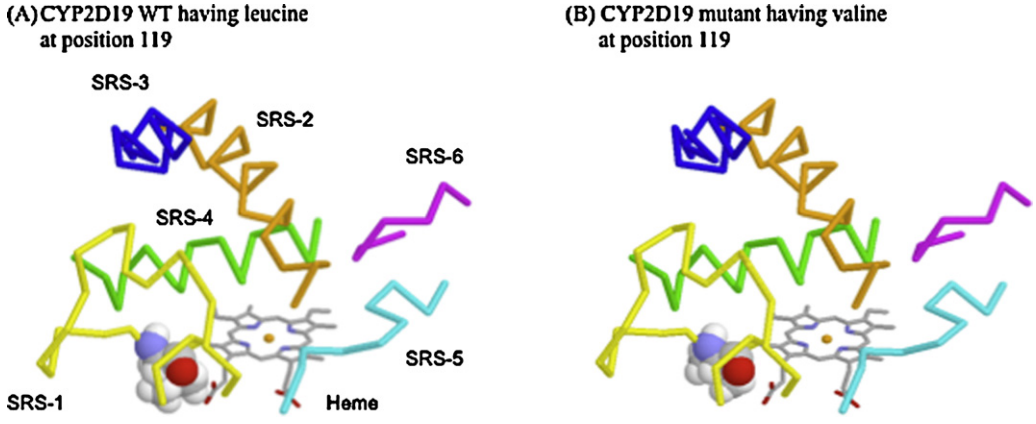

Fig. 6. Comparison of the active-site structure between the CYP2D19 wild type having leucine (A) and its mutant having valine (B) at position 119. The active-site structure consists of six SRSs and the heme moiety. A space-filling model is used to depict the amino acid residue at position 119.

tiomers were mainly oxidized to 4-OH-PL, followed by 5-OH-PL and NDP by all of the enzymes. In kinetic analysis, apparent K_m values were similar and substrate enantioselectivity of *R*-PL < *S*-PL was observed in both K_m and V_{max} values for the three metabolites formed from PL enantiomers. The NDP-forming activity tended to be higher in the monkey enzymes, particularly CYP2D17, than in the human enzyme. These results indicate that in the oxidation of PL enantiomers by CYP2D enzymes, stereoselectivity is similar but some differences exist in regioselectivity between humans and monkeys.

Conflict of interest

The author declares that there are no conflicts of interest.

References

[1] W.E. Evans, M.V. Relling, Pharmacogenomics: translating functional genomics into rational therapeutics, Science 286 (1999) 487–491.
[2] The home page of Dr. David Nelson; http://drnelson.uthsc.edu/CytochromeP450.html.
[3] S. Rendic, F.J. Di Carlo, Human cytochrome P450 enzymes: a status report summarizing their reactions, substrates, inducers and inhibitors, Drug Metab. Rev. 29 (1997) 413–580.
[4] U.M. Zanger, M. Turpeinen, K. Klein, M. Schwarb, Functional pharmacogenetics/genomics of human cytochrome P450 involved in drug biotransformation, Anal. Bioanal. Chem. 392 (2008) 1093–1108.
[5] T. Shimada, H. Yamazaki, M. Mimura, Y. Inui, F.P. Guengerich, Interindividual variations in human liver cytochrome P-450 enzymes involved in the oxidation of drugs, carcinogens and toxic chemicals: studies with liver microsomes of 30 Japanese and 30 Caucasians, J. Pharmacol. Exp. Ther. 270 (1994) 414–423.
[6] Home page of the human cytochrome P450 (CYP) allele nomenclature committee. http://www.cypalleles.ki.se/cyp2d6.htm.
[7] D.C. Mankowski, K.J. Laddison, P.A. Christpherson, S. Ekins, D.J. Tweedie, M.P. Lawton, Molecular cloning, expression, and characterization of CYP2D17 from cynomolgus monkey liver, Arch. Biochem. Biophys. 372 (1999) 189–196.
[8] T. Igarashi, T. Sakuma, M. Isogai, R. Nagata, T. Kamataki, Marmoset liver cytochrome P450s: study for expression and molecular cloning of their cDNAs, Arch. Biochem. Biophys. 339 (1997) 85–91.
[9] H. Hichiya, S. Kuramoto, S. Yamamoto, S. Shinoda, N. Hanioka, S. Narimatsu, K. Asaoka, A. Miyata, S. Iwata, M. Nomoto, T. Satoh, K. Kiryu, N. Ueda, S. Naito, G.T. Tucker, S.W. Ellis, Cloning and functional expression of a novel marmoset cytochrome P450 2D enzyme, CYP2D30: comparison with the known marmoset CYP2D19, Biochem. Pharmacol. 68 (2004) 165–175.
[10] A. Barrret, V. Cullum, The biological properties of the optical isomers of propranolol and their effects on cardiac arrhysmias, Br. J. Pharmacol. 34 (1968) 443–455.
[11] Y. Masubuchi, S. Hosokawa, T. Horie, S. Ohmori, M. Kitada, T. Suzuki, S. Narimatsu, Cytochrome P-450 isozymes involved in propranolol metabolism in human liver microsomes: the role of CYP-2D6 as ring-hydroxylase and CYP1A2 as N-desisopropyrase, Drug Metab. Dispos. 22 (1994) 909–915.
[12] B. Silber, N.H. Holford, S. Riegelman, Stereoselective disposition and glucuronidation of propranolol in human, J. Pharm. Sci. 71 (1982) 699–704.
[13] T. Walle, U.K. Walle, D.R. Knapp, E.C. Conradi, E.M. Bargar, Identification of major sulfate conjugates in the metabolism of propranolol in dog and man, Drug Metab. Dispos. 11 (1983) 344–349.
[14] T. Shimizudani, K. Nagaoka, N. Hanioka, S. Yamano, S. Narimatsu, Comparative study of the oxidation of propranolol enantiomers in hepatic and small intestinal microsomes from cynomolgus and marmoset monkeys, Chemico-Biol. Interact. 183 (2010) 67–78.
[15] S. Narimatsu, M. Gotoh, Y. Masubuchi, T. Horie, S. Ohmori, M. Kitada, T. Kageyama, K. Asaoka, I. Yamamoto, T. Suzuki, Stereoselectivity in bunitrolol 4-hydroxylation in liver microsomes from marmosets and Japanese monkeys, Biol. Pharm. Bull. 19 (1996) 1429–1433.
[16] S. Narimatsu, M. Oda, H. Hichiya, T. Isobe, K. Asaoka, N. Hanioka, S. Yamano, S. Shinoda, S. Yamamoto, Molecular cloning and functional analysis of cytochrome P450 1A2 from Japanese monkey liver: comparison with marmoset cytochrome P450 1A2, Chemico-Biol. Interact. 152 (2005) 1–12.
[17] T. Omura, R. Sato, The carbon monoxide-binding pigment of liver microsomes I. Evidence for its hemoprotein nature, J. Biol. Chem. 239 (1964) 2370–2378.
[18] F.P. Guengerich, P. Wang, N.K. Davidson, Estimation of isozymes of microsomal cytochrome P-450 in rats, rabbits, and humans using immunochemical staining coupled with sodium dodecyl sulfate-polyacrylamide gel electrophoresis, Biochemistry 21 (1982) 1698–1706.
[19] O.H. Lowry, N.J. Rosebrough, A.L. Farr, R.J. Randall, Protein measurement with the Folin phenol reagent, J. Biol. Chem. 193 (1951) 265–275.
[20] K. Masuda, K. Tamagake, Y. Okuda, F. Torigoe, D. Tsuzuki, T. Isobe, H. Hichiya, N. Hanioka, S. Yamamoto, S. Narimatsu, Change in enantioselectivity in bufuralol 1″-hydroxylation by the substitution of phenylalanine-120 by alanine in cytochrome P450 2D6, Chirality 17 (2005) 37–43.
[21] Y. Uno, S. Uehara, S. Kohara, N. Murayama, H. Yamazaki, Cynomolgus monkey CYP2D44 newly identified in liver, metabolizes bufuralol and dextromethorphan, Drug Metab. Dispos. (2010), Fast forward, published on May 25 as doi:10.112/dmd.110.033274.
[22] T. Omura, R. Sato, The carbon monoxide-binding pigment of liver microsomes II. Solubilization, purification and properties, J. Biol. Chem. 239 (1964) 2379–2385.